Monitoring statistics of the ERS-2 scatterometer for ESA

Cycle 130

(Project Ref. 18212/04/I-OL)

Hans Hersbach
European Centre for Medium-Range Weather Forecasts,
Shinfield Park, Reading, RG2 9AX, England
Tel: (+44 118) 9499476, e-mail: dal@ecmwf.int

November 5, 2007

1 Introduction

The quality of the UWI product was monitored at ECMWF for Cycle 130. Results were compared to those obtained from the previous Cycle, as well for data received during the nominal period in 2000 (up to Cycle 59). No corrections for duplicate observations were applied.

During Cycle 130 data was received between 21:01 UTC 24 September 2007 and 20:26 UTC 29 October 2007. Received data was grouped into 6-hourly batches (centred around 00, 06, 12 and 18 UTC). No data was received for the batch of 06 UTC 11 October 2007. Data is being recorded whenever within the visibility range of a ground station. From 1 October 2007 onwards data from Hobart station data was received again. On 18 October 2007, first data was received from a new station at Chetumal in Mexico, which extends coverage somewhat more westwards in the East Pacific. Quality of the data obtained from Hobart and Chetumal were found nominal. For Cycle 130, data coverage was over the North-Atlantic, the Mediterranean, the Gulf of Mexico, a small part of the Pacific west from the US, Canada and Central America, the Chinese Sea, a small part of the Indian Ocean South-East of Thailand and Indonesia, and the Southern Ocean close to the Antarctic and south of Australia and New Zealand (see Figure 2).

The asymmetry between the fore and aft incidence angles did not show large peaks.

Compared to Cycle 129, the UWI wind speed relative to ECMWF first-guess (FG) fields showed a slightly higher standard deviation (1.46 m/s, was 1.39 m/s). Bias levels were basically unaltered (on average -0.91 m/s, was -0.92 m/s).

Ocean calibration shows that inter-node and inter-beam dependencies of bias levels are large, though reduced compared to the situation for Cycle 128. Average bias levels were 0.17 dB less negative (-0.58 dB, was -0.75 dB; see Figure 4).

The ECMWF assimilation and forecast system was not changed during Cycle 130.

The Cycle-averaged evolution of performance relative to ECMWF first-guess (FG) winds is displayed in Figure 1. Figure 2 shows global maps of the over Cycle 130 averaged UWI data coverage and wind climate, Figure 3 for performance relative to FG winds.

2 ERS-2 statistics from 24 September to 29 October 2007

2.1 Sigma0 bias levels

The average sigma0 bias levels (compared to simulated sigma0's based on ECMWF model FG winds) stratified with respect to antenna beam, ascending or descending track and as function of incidence angle (i.e. across-node number) is displayed in Figure 4.

Inter-node and inter-beam dependencies have improved compared to Cycle 129, and are similar to those for a similar period one year ago (see Cyclic report 120). The gap between the fore/aft and mid beam is still large (especially for the ascending tracks). Average bias levels are less negative (-0.58 dB, was -0.75 dB), being around 0.20 dB more negative than for nominal data in 2000 (around -0.4 dB; see Figure 1 of the reports for Cycle 48 to 59).

Long-term variations correlate with the yearly cycle, which, given the non-global coverage, is understandable. Therefore, the method of ocean calibration will probably only provide accurate information on calibration levels for globally or yearly averaged data sets.

The data volume of descending tracks was about 21% higher than for ascending tracks.

2.2 Incidence angles

For ESACA, across-node binning is, like the old processor, retained on a 25km mesh. From simple geometrical arguments it follows that variations in yaw attitude will lead to asymmetries between the incidence angles of the fore and aft beam. Indeed, this has been observed. Figure 5 gives a time evolution of this asymmetry. Also in this Figure, the occasions for which the combined k_p-yaw quality flag was set are indicated by red stars. The relation with incidence-angle asymmetries is obvious.

No large peaks occurred during cycle 130. Solar activity has been low during this period, though the Earth was hit by a high-speed solar wind stream between 28 September and 2 October 2007 (source: www.spaceweather.com).

2.3 Distance to cone history

The distance to the cone history is shown in Figure 6. Curves are based on data that passed all QC, including the test on the k_p-yaw flag, and subject to the land and sea-ice check at ECMWF (see cyclic report 88 for details).

Like for Cycle 129, time series are (due to lack of statistics) very noisy, especially for the near-range nodes. Most spikes were found to be the result of low data volumes. After the data void on 11 October 2007, the distance to the cone seems reduced for the near-range nodes.

Compared to Cycle 129, the average level was lower (1.17 versus 1.22), however, higher (by 7%) than for nominal data (see top panel Figure 1).

The fraction of data that did not pass QC is displayed in Figure 6 as well (dashed curves).

2.4 UWI minus First-Guess wind history

In Figure 7, the UWI minus ECMWF first-guess wind-speed history is plotted.

The history plot shows a few peaks, which are usually the result of low data volume.

Figure 11 displays the locations for which UWI winds were more than 8 m/s weaker (top panel), respectively more than 8 m/s stronger (lower panel) than FG winds. Like for Cycle 129, such collocations are isolated, and often indicate meteorologicaly active regions, for which UWI data and ECMWF model field show reasonably small differences in phase and/or intensity. Deviations near the poles are the result of imperfect sea-ice flagging.

Two examples for a mismatch between ECMWF and UWI winds are the capture of two low-pressure systems, one south-east from New Zealand on 13 October 2007 (top panel), and one south off the Mexican coast on 18 October 2007 (lower panel). The case near New Zealand, which was acquired by Hobart station, shows some differences in the shape of the elongated low between model and scatterometer winds. The UWI winds clearly suffer from some de-aliasing problems. For the case in the East Pacific, close to Mexico, ERS-2 shows a patch of strong westerly winds with nearly constant wind direction, where the ECMWF model winds have a more circular flow around the pressure minimum.

Average bias levels and standard deviations of UWI winds relative to FG winds are displayed in Table 1. From this it follows that the bias of UWI winds was very similar (-0.91 m/s, was -0.92 m/s), being around -0.1 m/s more negative than for nominal data in 2000.

On a longer time scale seasonal bias trends are observed (see Figure 1). As was highlighted in previous cyclic reports, it is believed that this yearly trend is partly induced by changing local geophysical conditions. Strong indication for this is a similar trend observed for QuikSCAT data when restricted to an area well-covered by ERS-2 (20N-90N, 80W-20E). Figure 17 shows time series for that area for both ERS-2 (top panel) and QuikSCAT (lower panel) for the period between 1 January 2004 and 29 October 2007 (end of Cycle 130). Results are displayed for at ECMWF

	Cycle 129		Cycle 130	
	UWI	CMOD4	UWI	CMOD4
speed STDV	1.39	1.39	1.46	1.46
node 1-2	1.40	1.39	1.53	1.51
node 3-4	1.36	1.35	1.44	1.43
node 5-7	1.33	1.32	1.40	1.40
node 8-10	1.35	1.35	1.43	1.42
node 11-14	1.37	1.37	1.44	1.44
node 15-19	1.39	1.40	1.44	1.45
speed BIAS	-0.92	-0.93	-0.91	-0.91
node 1-2	-1.42	-1.40	-1.43	-1.40
node 3-4	-1.21	-1.17	-1.18	-1.14
node 5-7	-0.98	-0.95	-0.94	-0.91
node 8-10	-0.79	-0.79	-0.76	-0.76
node 11-14	-0.72	-0.74	-0.72	-0.74
node 15-19	-0.72	-0.76	-0.73	-0.77
direction STDV	28.7	19.6	35.6	19.6
direction BIAS	-2.4	-2.4	-1.4	-1.9

Table 1: Biases and standard deviation of ERS-2 versus ECMWF FG winds in m/s for speed and degrees for direction.

actively assimilated data, i.e., CMOD5 winds for ERS-2 and 4%-reduced QuikSCAT winds on a 50km resolution. Note the increase in wind speed for ERS-2 since the introduction of the new model cycle at ECMWF on 7 June 2007. It reflects the switch from the CMOD5 to CMOD5.4 model function, which has increased ERS-2 wind speed by 0.48 m/s.

The standard deviation of UWI wind speed versus ECMWF FG was, compared to Cycle 129, somewhat higher (1.46 m/s, was 1.39 m/s).

For Cycle 130 the (UWI - FG) direction standard deviations were mostly ranging between 20 and 40 degrees (Figure 8), representing nominal variations. However, between 25 and 27 October 2007, the performance was severely reduced. Since no reduction was observed for at ECMWF de-aliased winds, it indicates temporal problems in the de-aliasing procedure in the UWI processing. Averaged over the entire cyclic period, STDV for UWI wind direction has increased (35.6 degrees, was 28.7 degrees), mainly induced by the two-day anomalous period. For at ECMWF de-aliased winds no trend was observed (STDV 19.6 degrees, unchanged).

2.5 Scatterplots

Scatterplots of FG winds versus ERS-2 winds are displayed in Figures 13 to 16. Values of standard deviations and biases are slightly different from those displayed in Table 1. Reason for this is that, for plotting purposes, the in 0.5 m/s resolution ERS-2 winds have been slightly perturbed (increases scatter with 0.02 m/s), and that zero wind-speed ERS-2 winds have been excluded (decreases scatter by about

0.05 m/s).

The scatterplot of UWI wind speed versus FG (Figure 13) is very similar to that for (at ECMWF inverted) de-aliased CMOD4 winds (Figure 15). It confirms that the ESACA inversion scheme is working properly.

Winds derived on the basis of CMOD5 are displayed in Figure 16. The relative standard deviation is lower than for CMOD4 winds (1.44 m/s versus 1.48 m/s). Compared to ECMWF FG, CMOD5 winds are 0.41 m/s slower.

Figure Captions

Figure 1: Evolution of the performance of the ERS-2 scatterometer averaged over 5-weekly Cycles from 12 December 2001 (Cycle 69) to 29 October 2007 (end Cycle 130) for the UWI product (solid, star) and de-aliased winds based on CMOD4 (dashed, diamond). Results are based on data that passed the UWI QC flags. For Cycle 85 two values are plotted; the first value for a global set, the second one for a regional set (for details see the corresponding cyclic report). Dotted lines represent values for Cycle 59 (5 December 2000 to 17 January 2001), i.e. the last stable Cycle of the nominal period. From top to bottom panel are shown the normalized distance to the cone (CMOD4 only) the standard deviation of the wind speed compared to FG winds, the corresponding bias (for UWI winds the extremes in node-wise averages are shown as well), and the standard deviation of wind direction compared to FG.

Figure 2: Average number of observations per 12H and per 125km grid box (top panel) and wind climate (lower panel) for UWI winds that passed the UWI flags QC and a check on the collocated ECMWF land and sea-ice mask.

Figure 3: The same as Figure 2, but now for the relative bias (top panel) and standard deviation (lower panel) with ECMWF first-guess winds.

Figure 4: Ratio of $< \sigma_0^{0.625} > / <$ CMOD4(FirstGuess)$^{0.625} >$ converted in dB for the fore beam (solid line), mid beam (dashed line) and aft beam (dotted line), as a function of incidence angle for descending and ascending tracks. The thin lines indicate the error bars on the estimated mean. First-guess winds are based on the in time closest (+3h, +6h, +9h, or +12h) T799 forecast field, and are bilinearly interpolated in space.

Figure 5: Time series of the difference in incidence angle between the fore and aft beam. Red stars indicate the occurrences for which the combined k_p-yaw flag was set.

Figure 6: Mean normalized distance to the cone computed every 6 hours for nodes 1-2, 3-4, 5-7, 8-10, 11-14 and 15-19). The dotted curve shows the number of incoming triplets in logarithmic scale (1 corresponds to 60,000 triplets) and the dashed one indicates the fraction of complete (based on the land and sea-ice mask at ECMWF) sea-located triplets rejected by ESA flags, or by the wind inversion algorithm (0: all data kept, 1: no data kept).

Figure 7: Mean (solid line) and standard deviation (dashed line) of the wind speed difference UWI - first guess for the data retained by the quality control.

Figure 8: Same as Fig. 7, but for the wind direction difference. Statistics are computed for winds stronger than 4 m/s.

Figures 9 and 10: Same as Fig. 7 and 8 respectively, but for the de-aliased CMOD4 data.

Figure 11: Locations of data during Cycle 130 for which UWI winds are more than 8 m/s weaker (top panel) respectively stronger (lower panel) than FG, and on which QC on UWI flags and the ECMWF land/sea-ice mask was applied.

Figure 12: Comparison between UWI winds (in red) and ECMWF FG winds (in blue) for a case on 13 October 2007 south-east from New Zealand (top panel) and a case on 18 October south from Mexico (lower panel).

Figure 13: Two-dimensional histogram of first guess and UWI wind speeds, for the data kept by the UWI flags, and QC based on the ECMWF land and sea-ice mask. Circles denote the mean values in the y-direction, and squares those in the x-direction.

Figure 14: Same as Fig. 13, but for wind direction. Only winds stronger than 4m/s are taken into account.

Figure 15: Same as Fig. 13, but for de-aliased CMOD4 winds.

Figure 16: Same as Fig. 13, but for de-aliased CMOD5 winds.

Figure 17: Wind-speed bias relative to FG winds for actively assimilated ERS-2 winds (based on CMOD5 before 7 June 2007; CMOD5.4 afterwards) for nodes 1-19 (top panel) respectively 50-km QuikSCAT (based on the QSCAT-1 model function and reduced by 4%) for nodes 5-34 (lower panel), averaged over the area (20N-90N, 80W-20E), and displayed for the period 1 January 2004 - 29 October 2007. Fat curves represent centred 15-day running means, thin curves values for 6-hourly periods. Vertical dashed blue lines mark ECMWF model changes.

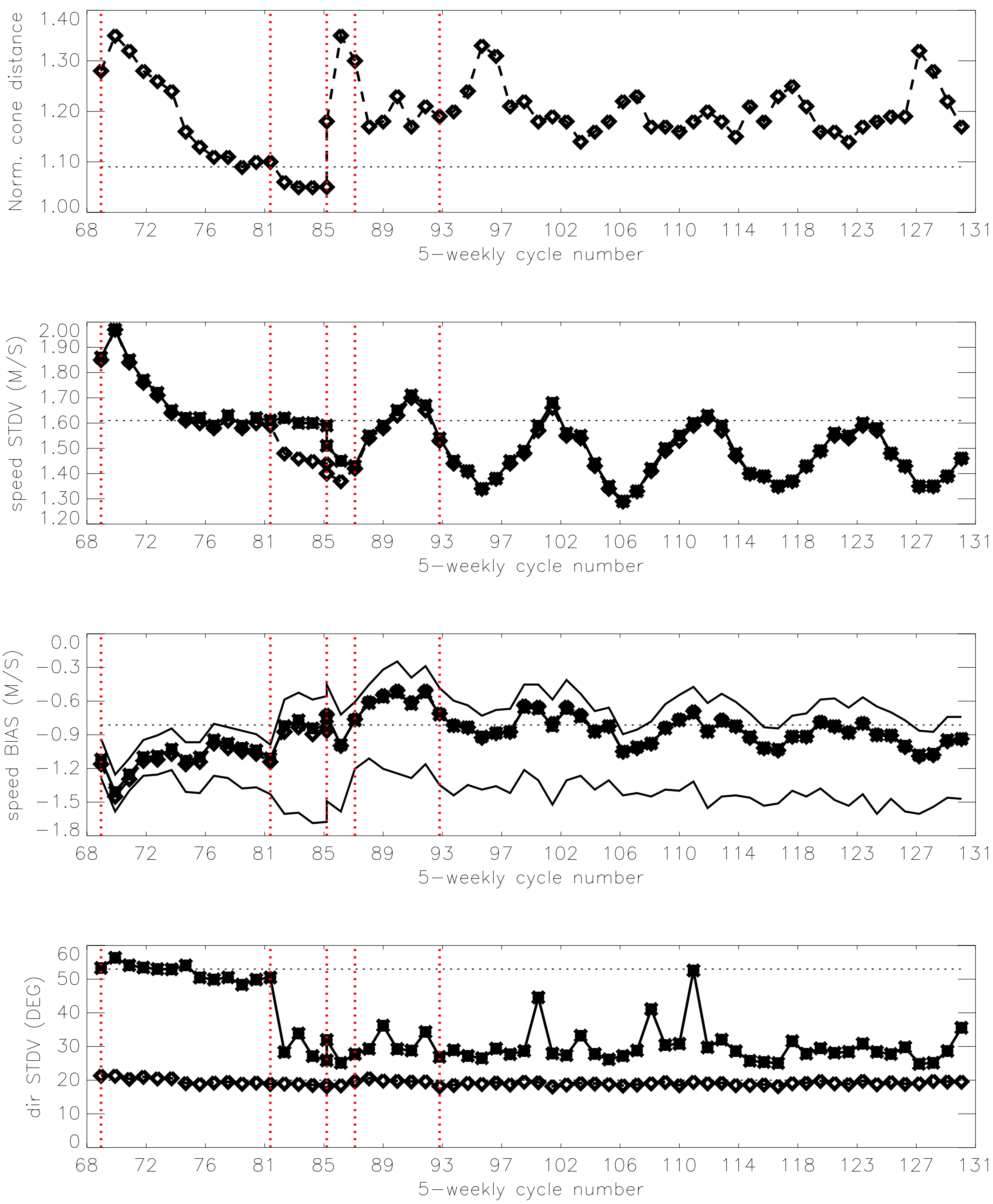
Norm. cone distance
speed STDV (M/S)
speed BIAS (M/S)
dir STDV (DEG)
5−weekly cycle number

Figure 1

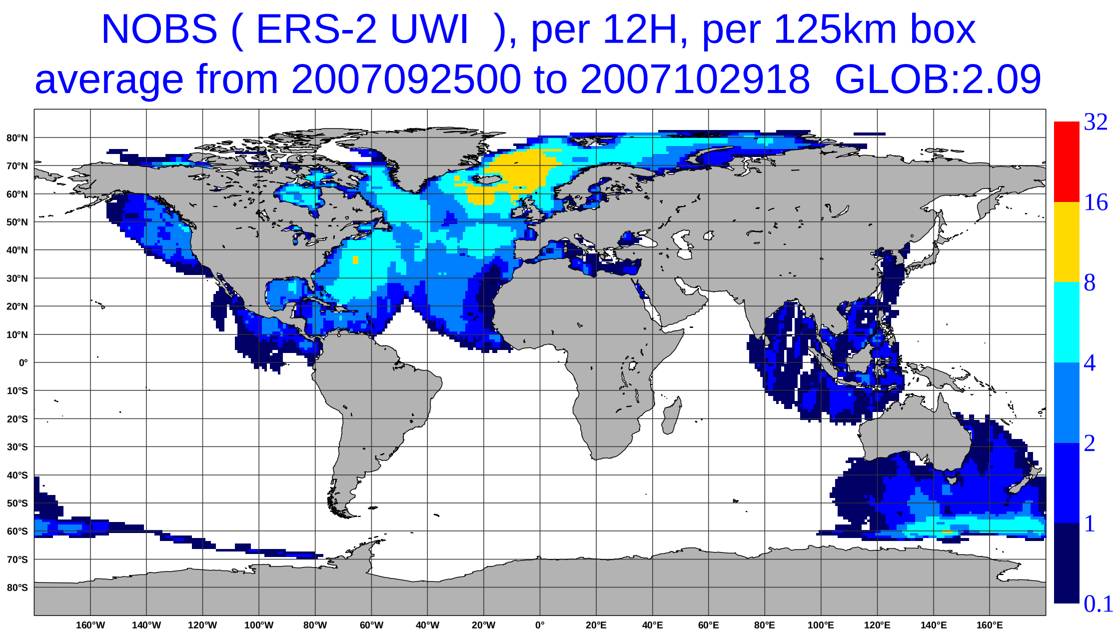
NOBS (ERS-2 UWI), per 12H, per 125km box
average from 2007092500 to 2007102918 GLOB:2.09
80°N
70°N
60°N
50°N
40°N
30°N
20°N
10°N
0°
10°S
20°S
30°S
40°S
50°S
60°S
70°S
80°S
160°W
140°W
120°W
100°W
80°W
60°W
40°W
20°W
0°
20°E
40°E
60°E
80°E
100°E
120°E
140°E
160°E
32
16
8
4
2
1
0.1

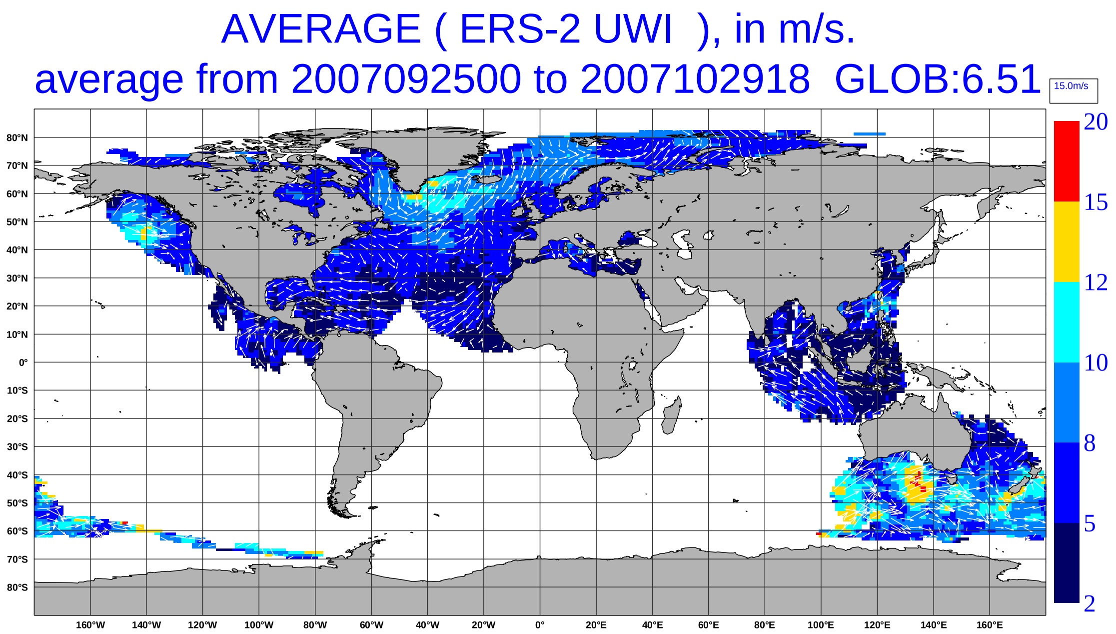
AVERAGE (ERS-2 UWI), in m/s.
average from 2007092500 to 2007102918 GLOB:6.51
15.0m/s
80°N
70°N
60°N
50°N
40°N
30°N
20°N
10°N
0°
10°S
20°S
30°S
40°S
50°S
60°S
70°S
80°S
160°W
140°W
120°W
100°W
80°W
60°W
40°W
20°W
0°
20°E
40°E
60°E
80°E
100°E
120°E
140°E
160°E
20
15
12
10
8
5
2

Figure 2

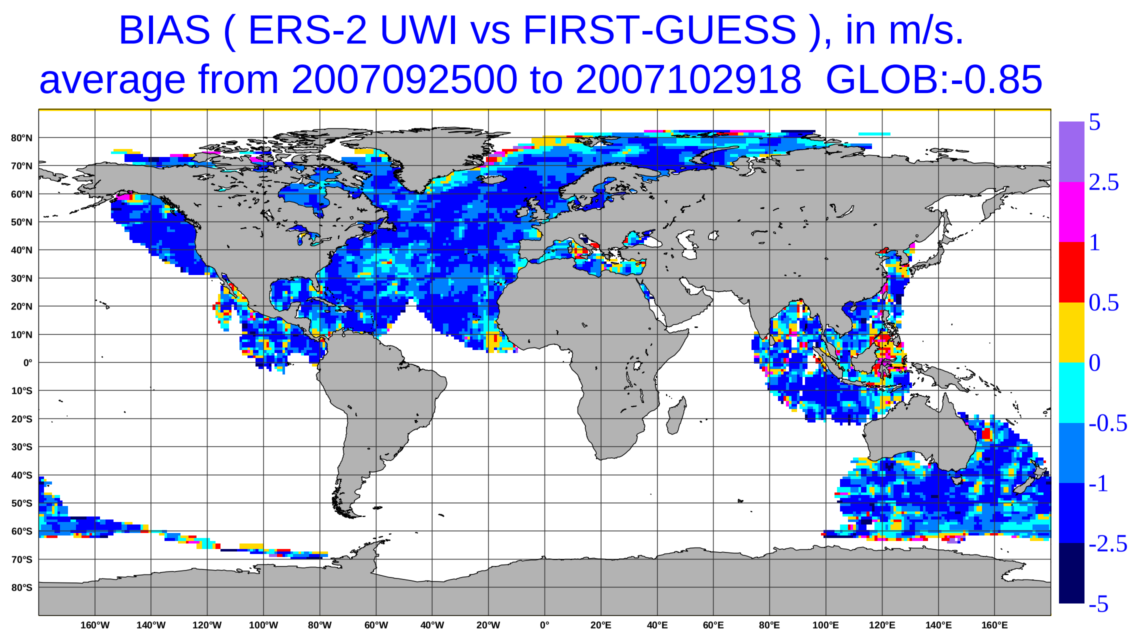
BIAS (ERS-2 UWI vs FIRST-GUESS), in m/s.
average from 2007092500 to 2007102918 GLOB:-0.85
80°N
70°N
60°N
50°N
40°N
30°N
20°N
10°N
0°
10°S
20°S
30°S
40°S
50°S
60°S
70°S
80°S
160°W
140°W
120°W
100°W
80°W
60°W
40°W
20°W
0°
20°E
40°E
60°E
80°E
100°E
120°E
140°E
160°E
5
2.5
1
0.5
0
-0.5
-1
-2.5
-5

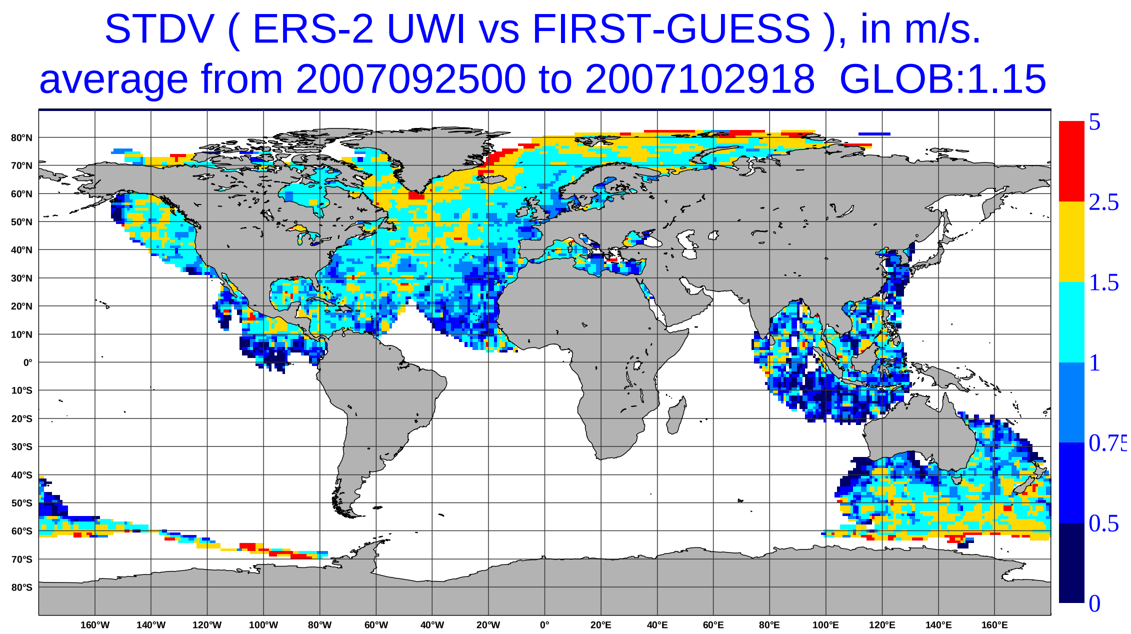
STDV (ERS-2 UWI vs FIRST-GUESS), in m/s.
average from 2007092500 to 2007102918 GLOB:1.15
80°N
70°N
60°N
50°N
40°N
30°N
20°N
10°N
0°
10°S
20°S
30°S
40°S
50°S
60°S
70°S
80°S
160°W
140°W
120°W
100°W
80°W
60°W
40°W
20°W
0°
20°E
40°E
60°E
80°E
100°E
120°E
140°E
160°E
5
2.5
1.5
1
0.5
0

Figure 3

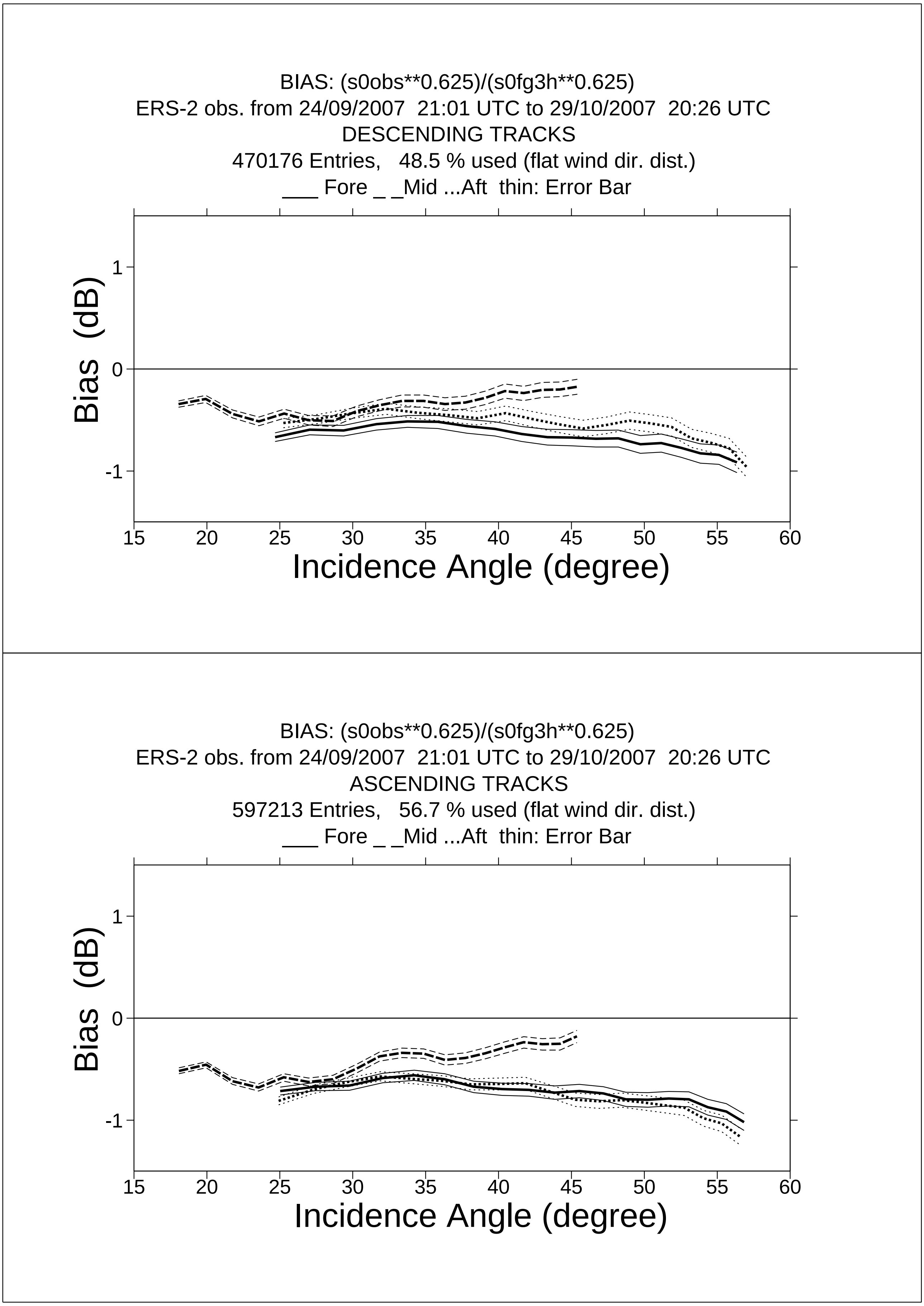
BIAS: (s0obs**0.625)/(s0fg3h**0.625)
ERS-2 obs. from 24/09/2007 21:01 UTC to 29/10/2007 20:26 UTC
DESCENDING TRACKS
470176 Entries, 48.5 % used (flat wind dir. dist.)
___ Fore _ _Mid ...Aft thin: Error Bar
Bias (dB)
1
0
-1
15
20
25
30
35
40
45
50
55
60
Incidence Angle (degree)
BIAS: (s0obs**0.625)/(s0fg3h**0.625)
ERS-2 obs. from 24/09/2007 21:01 UTC to 29/10/2007 20:26 UTC
ASCENDING TRACKS
597213 Entries, 56.7 % used (flat wind dir. dist.)
___ Fore _ _Mid ...Aft thin: Error Bar
Bias (dB)
1
0
-1
15
20
25
30
35
40
45
50
55
60
Incidence Angle (degree)

Figure 4

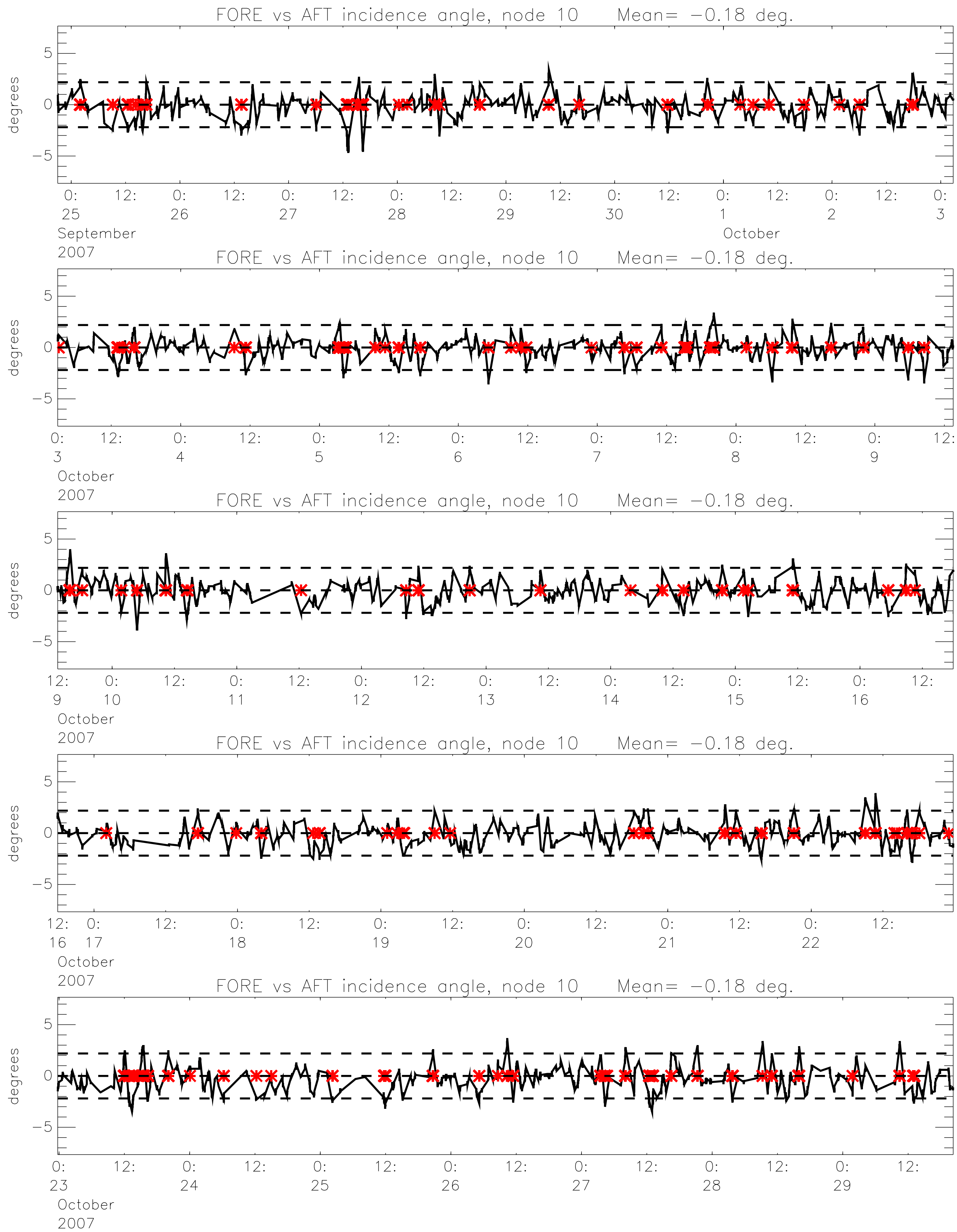
FORE vs AFT incidence angle, node 10 Mean= −0.18 deg.
degrees
September 2007
October
October 2007

Figure 5

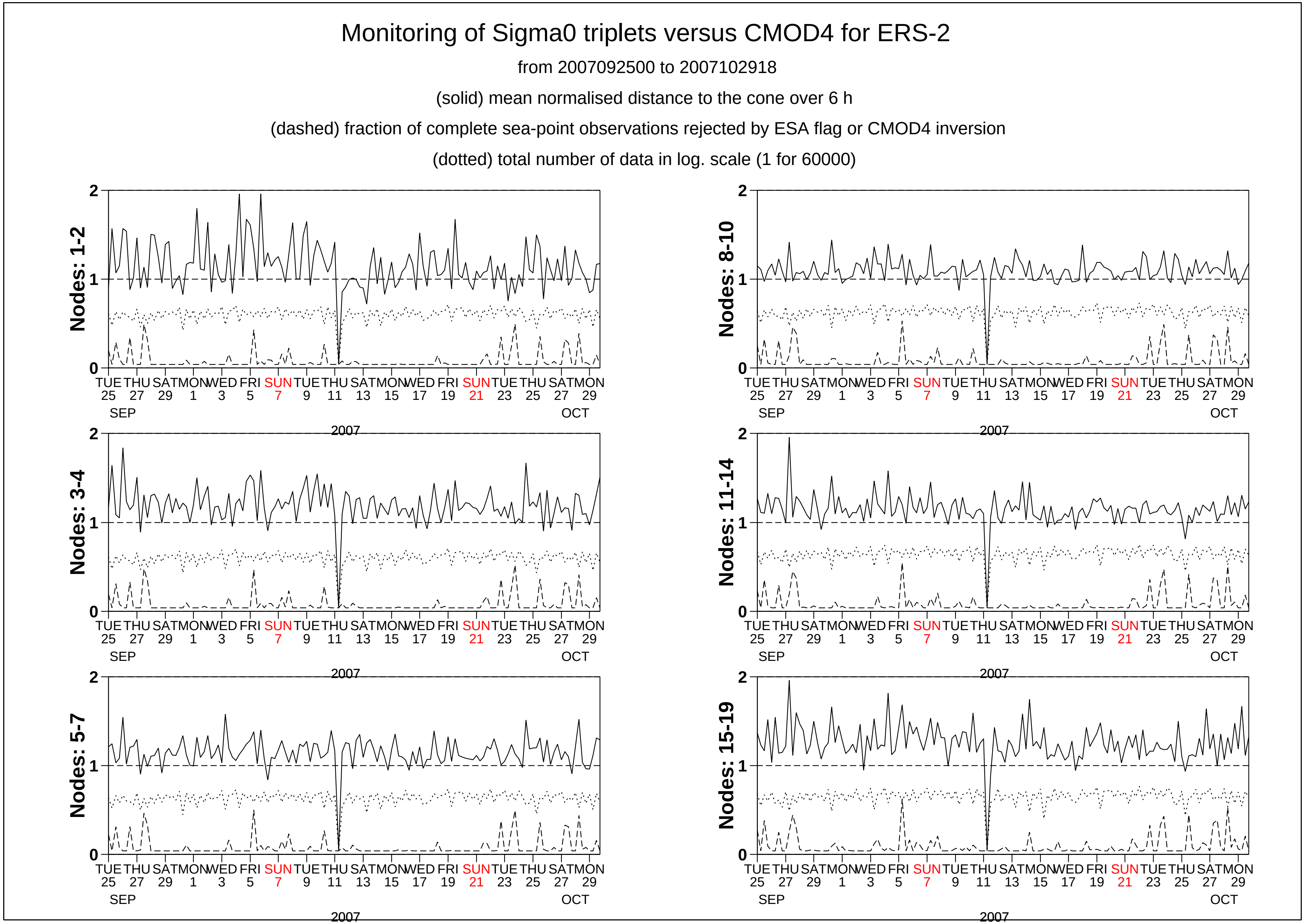
Monitoring of Sigma0 triplets versus CMOD4 for ERS-2
from 2007092500 to 2007102918
(solid) mean normalised distance to the cone over 6 h
(dashed) fraction of complete sea-point observations rejected by ESA flag or CMOD4 inversion
(dotted) total number of data in log. scale (1 for 60000)
Nodes: 1-2
Nodes: 8-10
Nodes: 3-4
Nodes: 11-14
Nodes: 5-7
Nodes: 15-19
TUE THU SAT MON WED FRI SUN TUE THU SAT MON WED FRI SUN TUE THU SAT MON
25 27 29 1 3 5 7 9 11 13 15 17 19 21 23 25 27 29
SEP OCT
2007

Figure 6

Monitoring of UWI winds versus First Guess for ERS-2

from 2007092500 to 2007102918

(solid) wind speed bias UWI - First Guess over 6h (deg.)

(dashed) wind speed standard deviation UWI - First Guess over 6h (deg.)

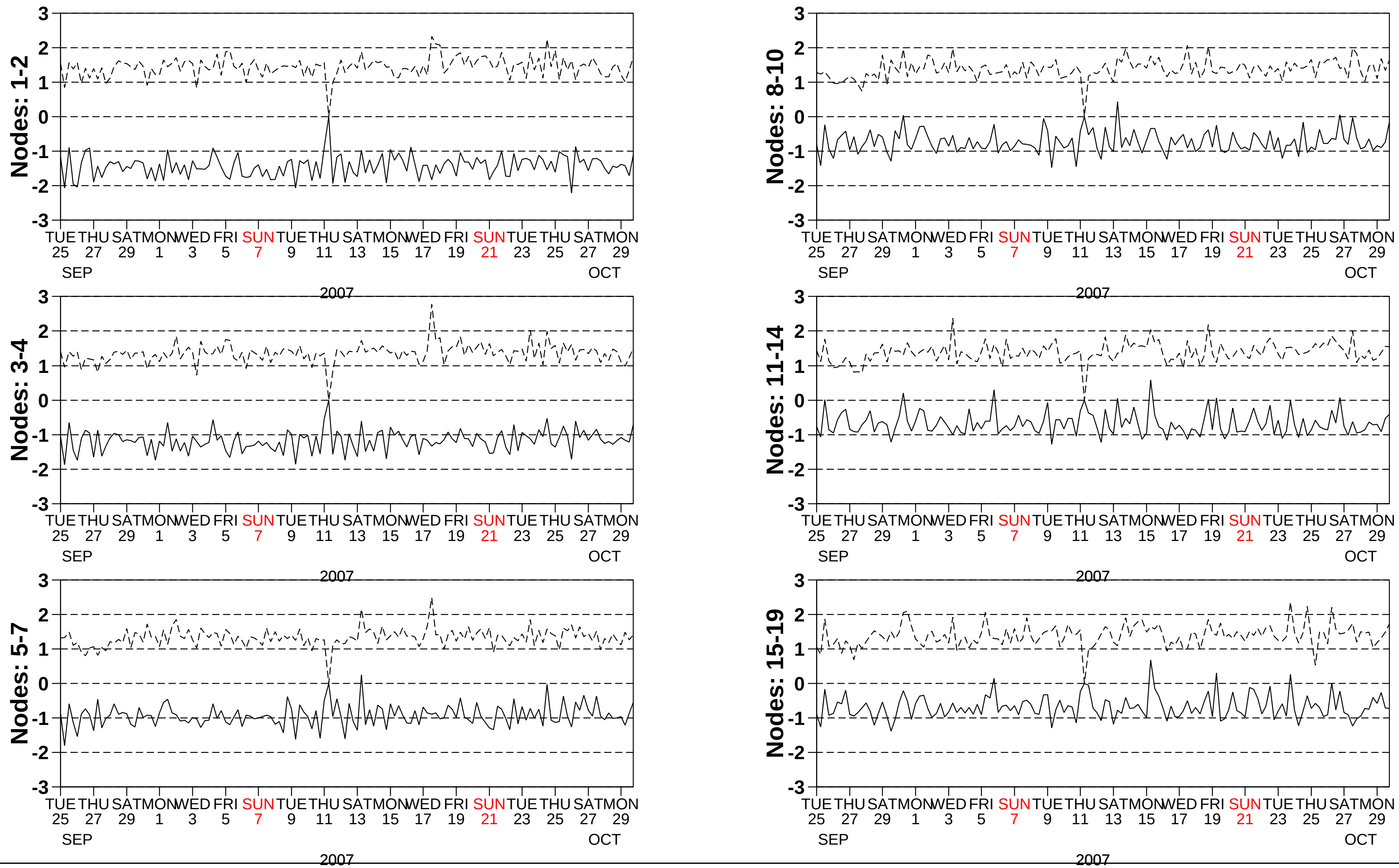

Figure 7

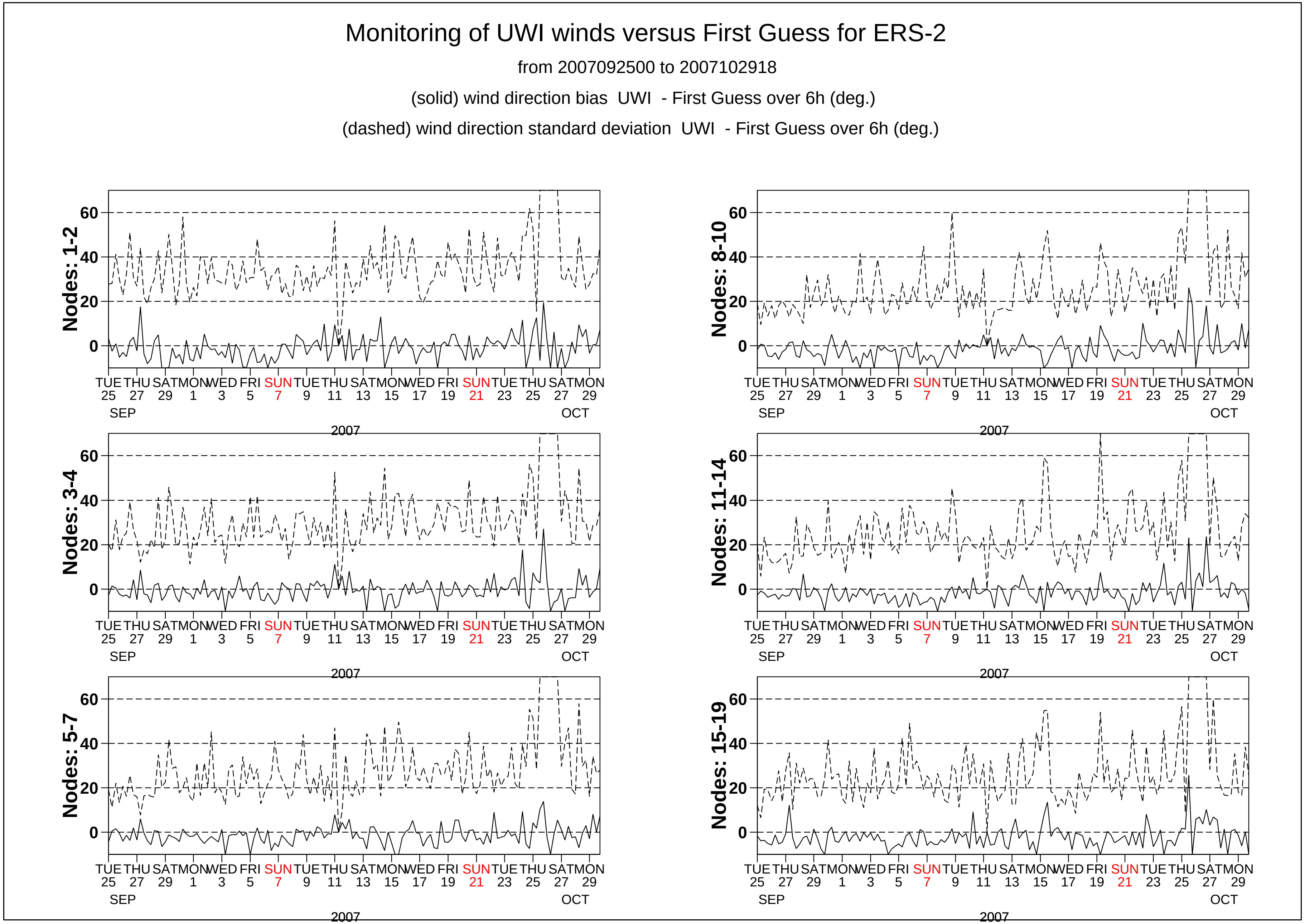
Monitoring of UWI winds versus First Guess for ERS-2
from 2007092500 to 2007102918
(solid) wind direction bias UWI - First Guess over 6h (deg.)
(dashed) wind direction standard deviation UWI - First Guess over 6h (deg.)
Nodes: 1-2
Nodes: 8-10
Nodes: 3-4
Nodes: 11-14
Nodes: 5-7
Nodes: 15-19
60
40
20
0
TUE THU SAT MON WED FRI SUN TUE THU SAT MON WED FRI SUN TUE THU SAT MON
25 27 29 1 3 5 7 9 11 13 15 17 19 21 23 25 27 29
SEP
OCT
2007

Figure 8

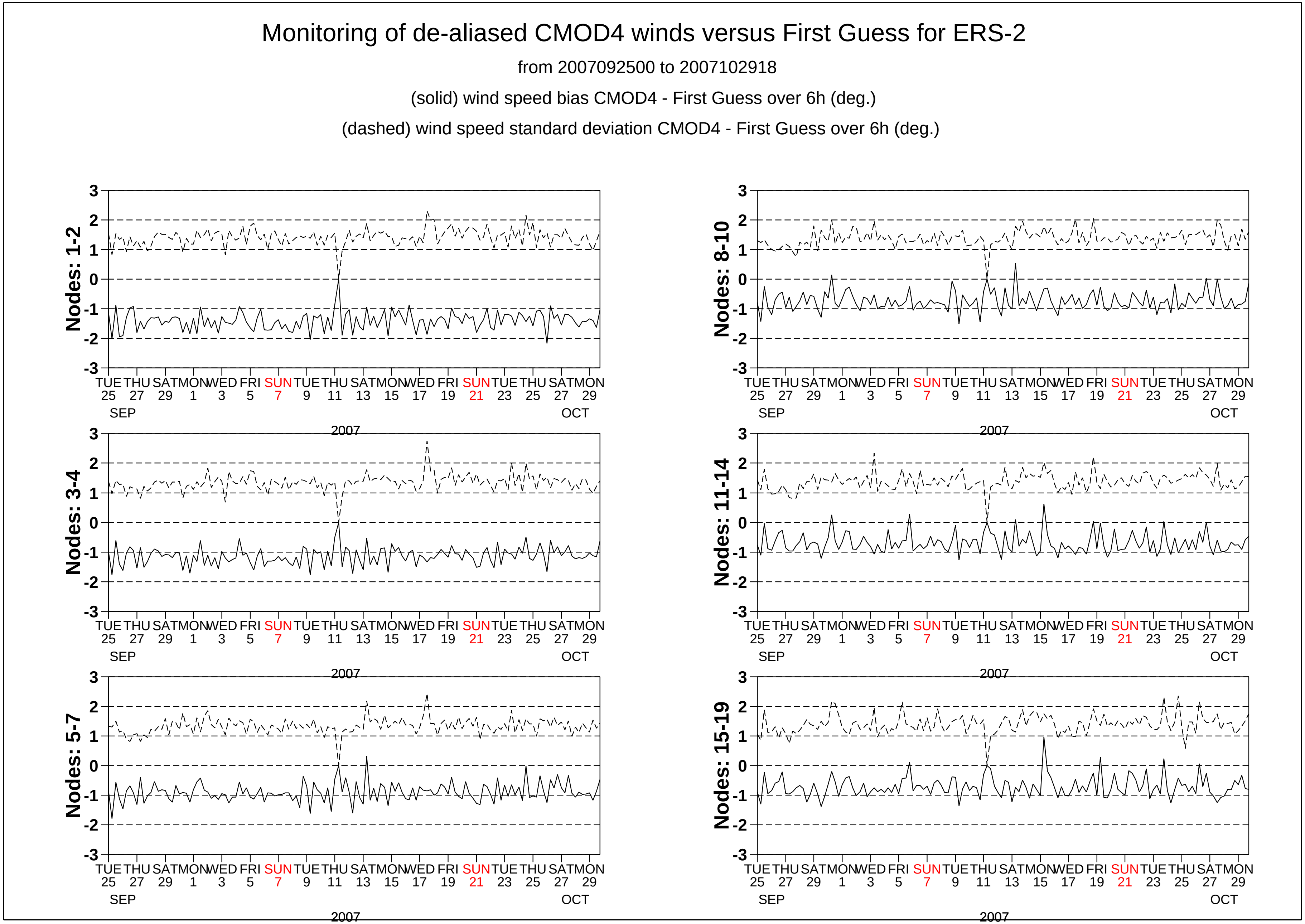
Monitoring of de-aliased CMOD4 winds versus First Guess for ERS-2
from 2007092500 to 2007102918
(solid) wind speed bias CMOD4 - First Guess over 6h (deg.)
(dashed) wind speed standard deviation CMOD4 - First Guess over 6h (deg.)
Nodes: 1-2
Nodes: 8-10
Nodes: 3-4
Nodes: 11-14
Nodes: 5-7
Nodes: 15-19
3
2
1
0
-1
-2
-3
TUE THU SAT MON WED FRI SUN TUE THU SAT MON WED FRI SUN TUE THU SAT MON
25 27 29 1 3 5 7 9 11 13 15 17 19 21 23 25 27 29
SEP
OCT
2007

Figure 9

Monitoring of de-aliased CMOD4 winds versus First Guess for ERS-2

from 2007092500 to 2007102918

(solid) wind direction bias CMOD4 - First Guess over 6h (deg.)

(dashed) wind direction standard deviation CMOD4 - First Guess over 6h (deg.)

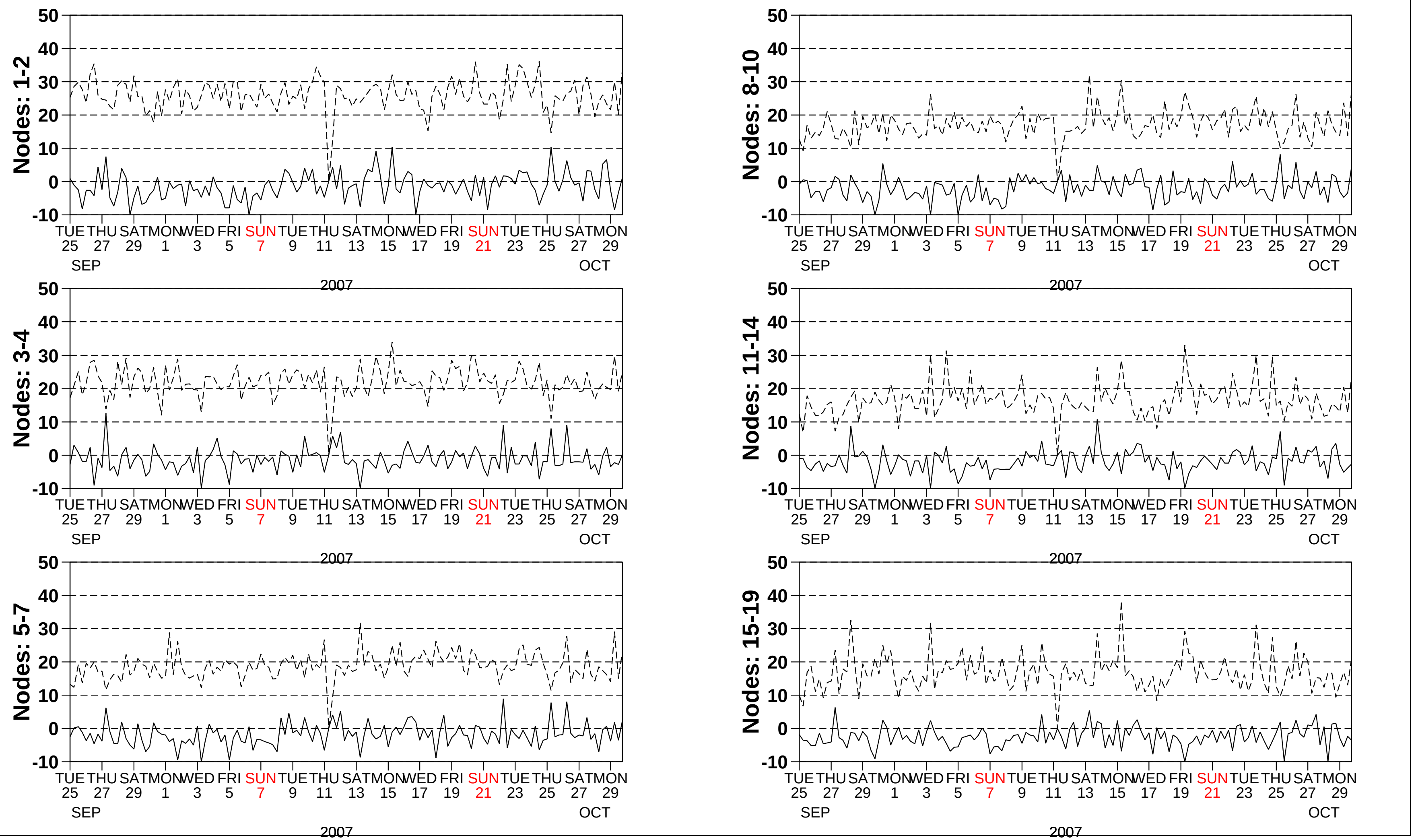

Figure 10

UWI winds more than 8 m/s weaker than ECMWF First Guess
CYCLE 130, 2007092500 to 2007102918, QC on ESA flags

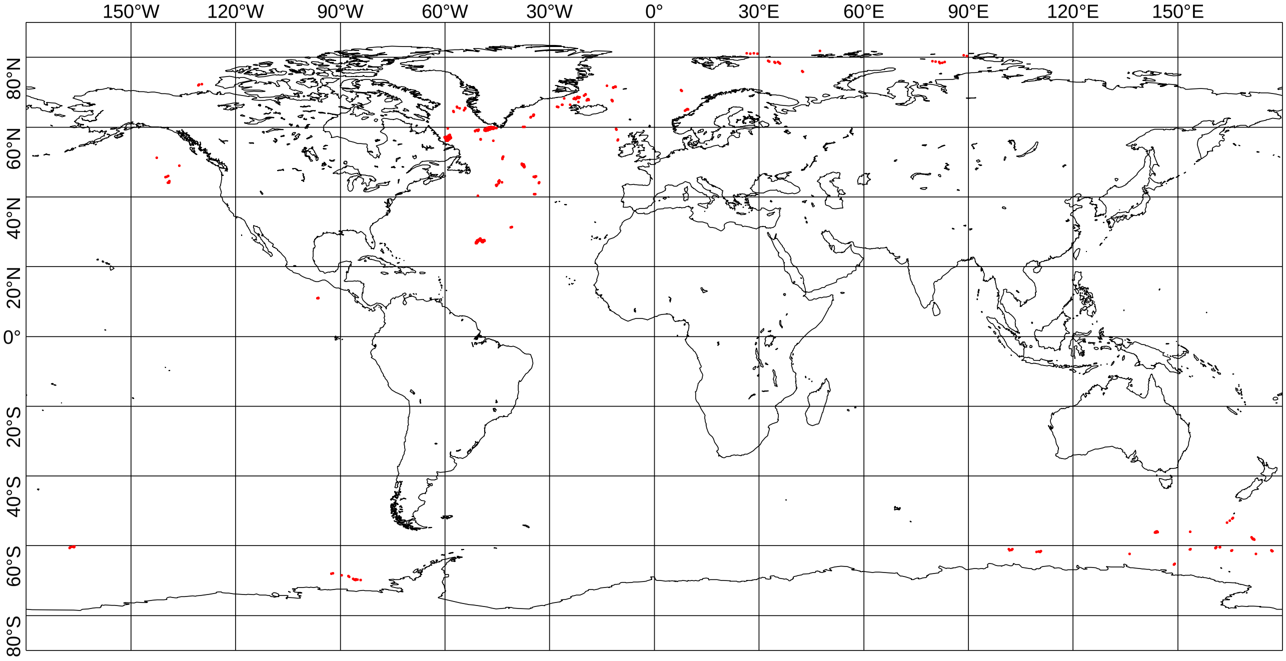

UWI winds more than 8 m/s stronger than ECMWF First Guess
CYCLE 130, 2007092500 to 2007102918, QC on ESA flags

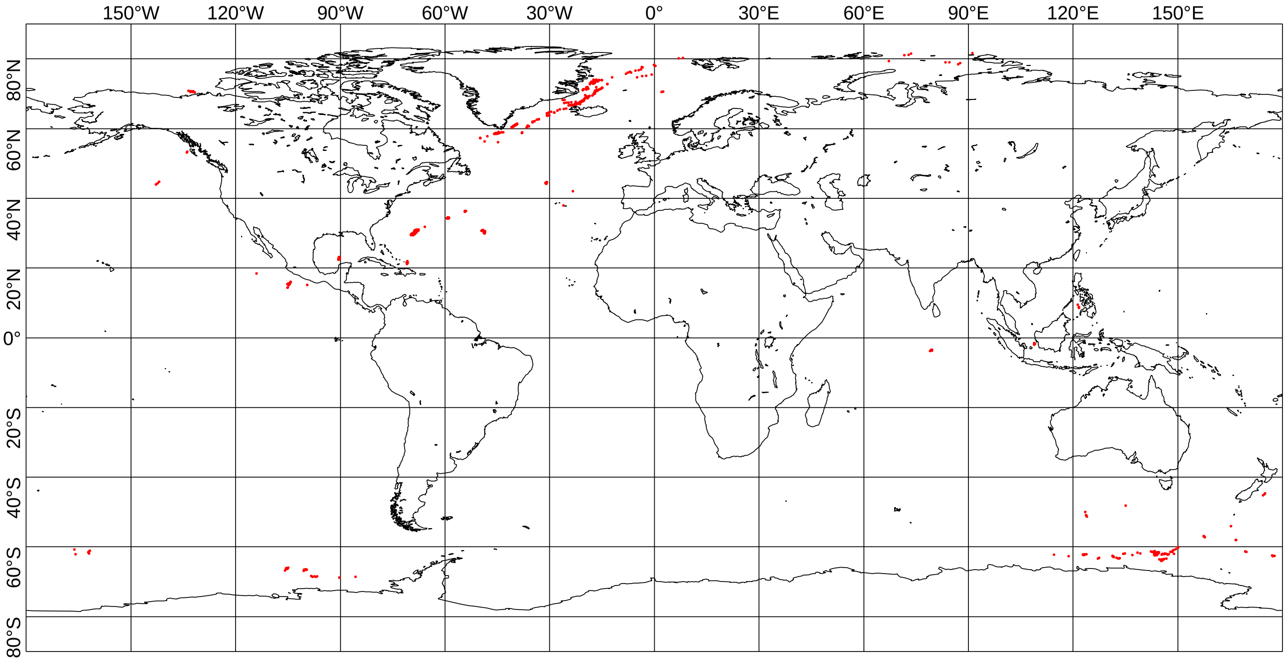

Figure 11

UWI winds (red) versus ECMWF FG winds (blue)
South-East off New Zealand 20071013 21:53 UTC

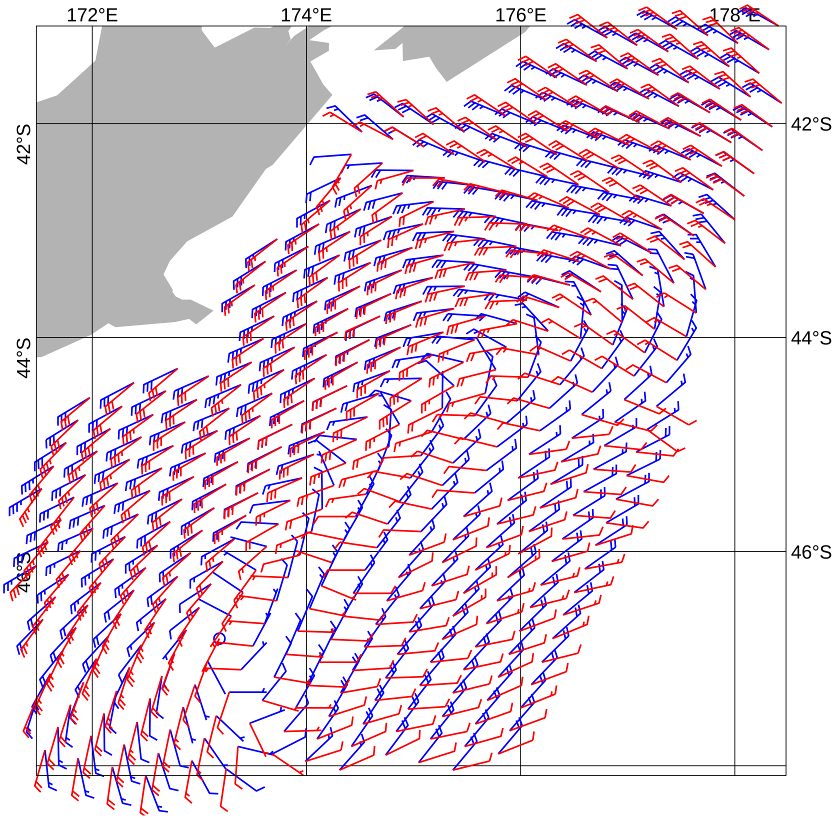

UWI winds (red) versus ECMWF FG winds (blue)
South off Mexico 20071018 17:17 UTC

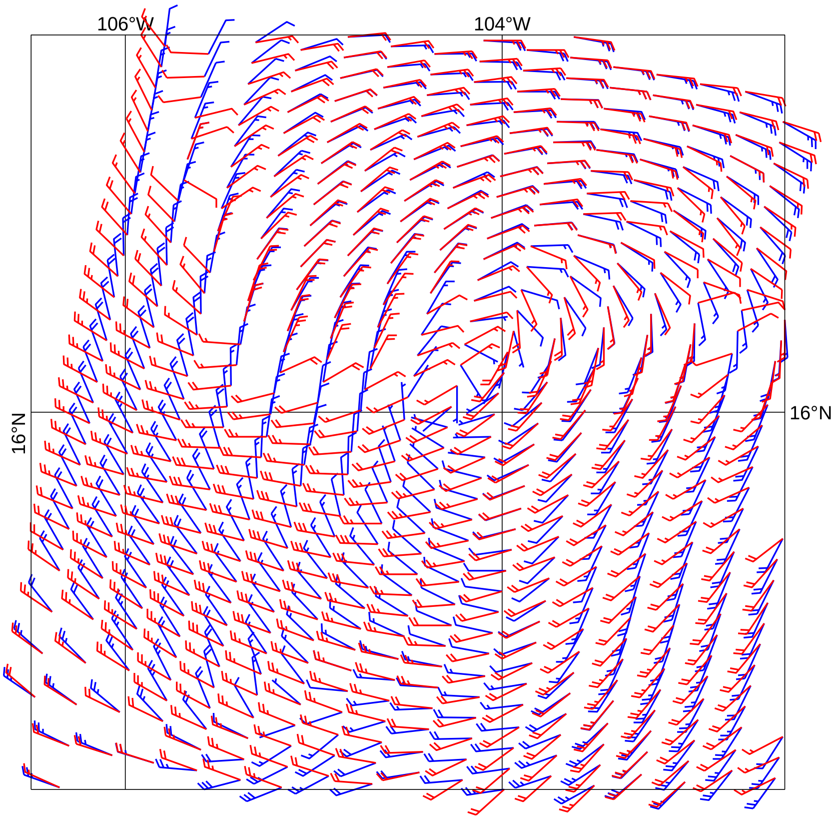

Figure 12

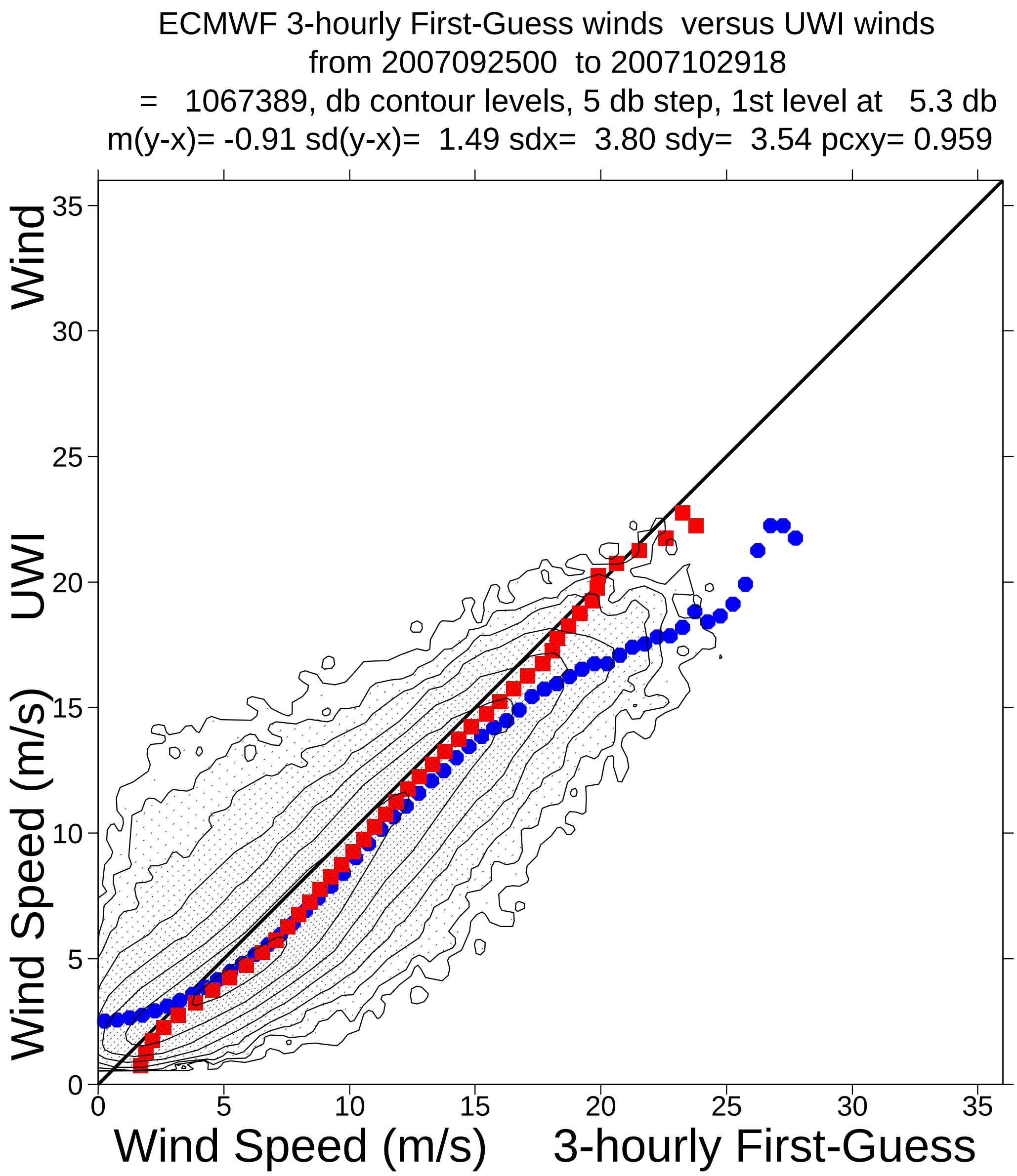
ECMWF 3-hourly First-Guess winds versus UWI winds
from 2007092500 to 2007102918
= 1067389, db contour levels, 5 db step, 1st level at 5.3 db
m(y-x)= -0.91 sd(y-x)= 1.49 sdx= 3.80 sdy= 3.54 pcxy= 0.959
Wind Speed (m/s) UWI Wind
Wind Speed (m/s) 3-hourly First-Guess
0
5
10
15
20
25
30
35

Figure 13

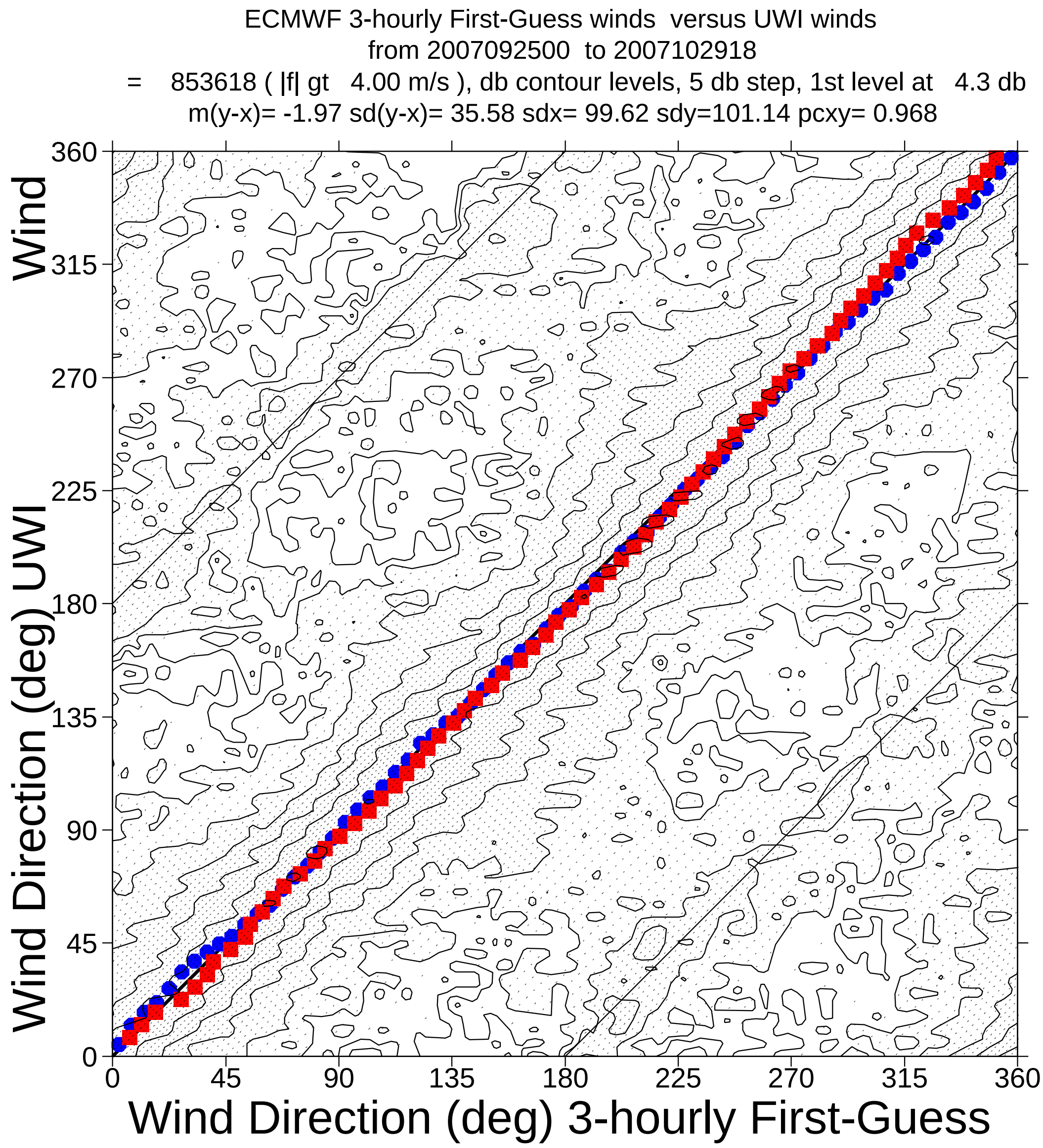
ECMWF 3-hourly First-Guess winds versus UWI winds
from 2007092500 to 2007102918
= 853618 (|f| gt 4.00 m/s), db contour levels, 5 db step, 1st level at 4.3 db
m(y-x)= -1.97 sd(y-x)= 35.58 sdx= 99.62 sdy=101.14 pcxy= 0.968
Wind
Wind Direction (deg) UWI
0
45
90
135
180
225
270
315
360
Wind Direction (deg) 3-hourly First-Guess

Figure 14

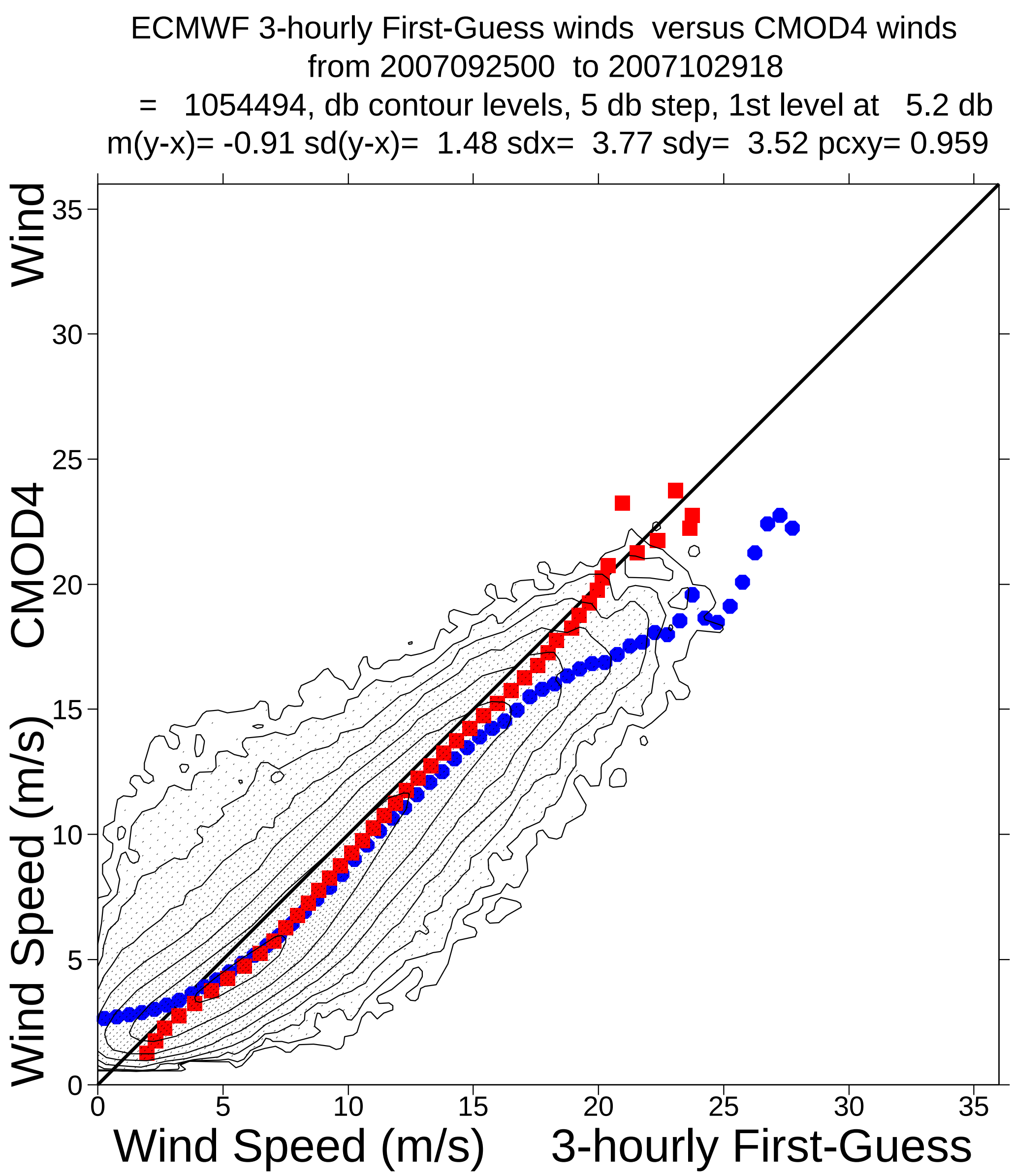

ECMWF 3-hourly First-Guess winds versus CMOD4 winds
from 2007092500 to 2007102918
= 1054494, db contour levels, 5 db step, 1st level at 5.2 db
m(y-x)= -0.91 sd(y-x)= 1.48 sdx= 3.77 sdy= 3.52 pcxy= 0.959
Wind Speed (m/s) CMOD4 Wind
Wind Speed (m/s) 3-hourly First-Guess
0
5
10
15
20
25
30
35

Figure 15

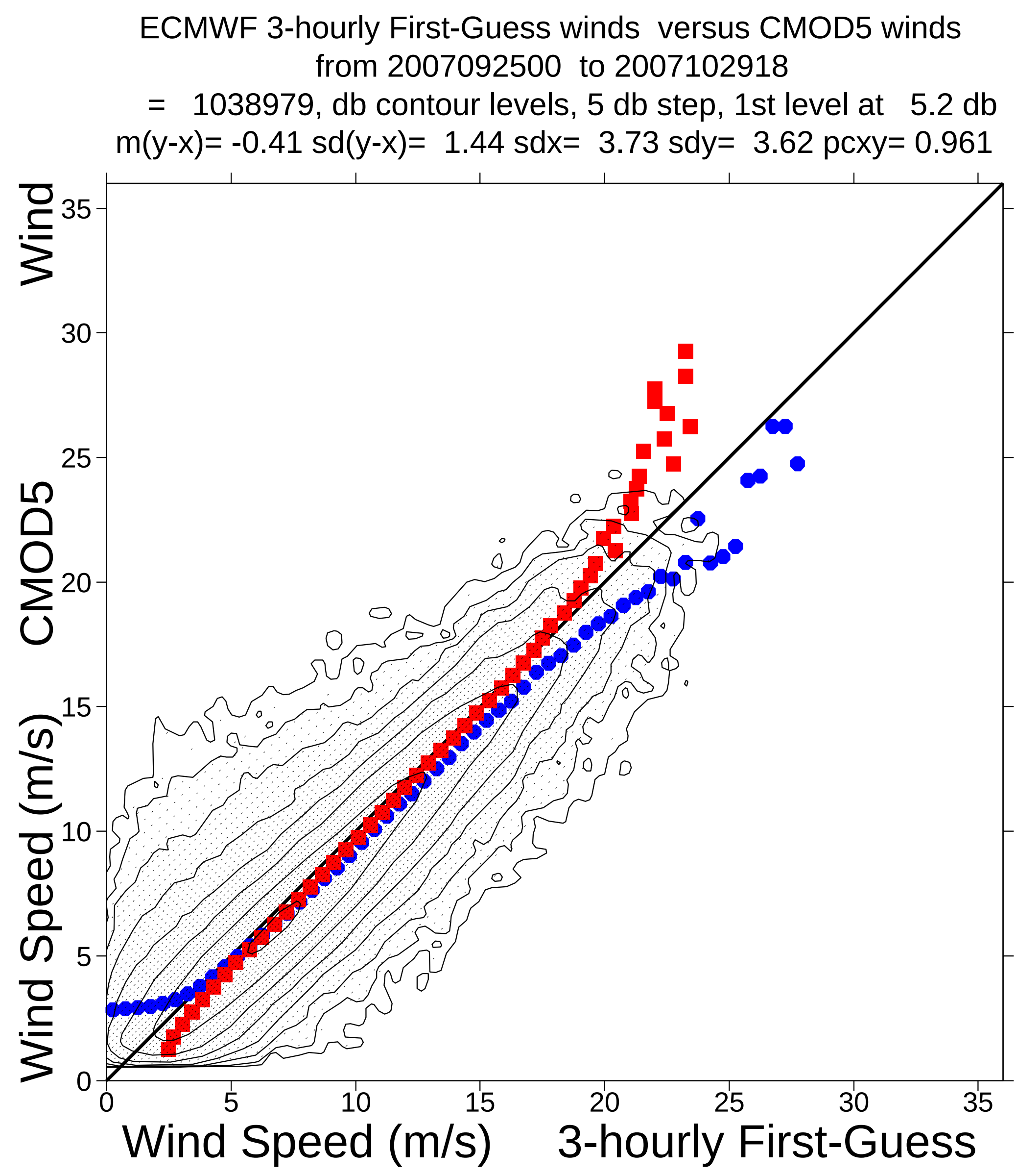
ECMWF 3-hourly First-Guess winds versus CMOD5 winds
from 2007092500 to 2007102918
= 1038979, db contour levels, 5 db step, 1st level at 5.2 db
m(y-x)= -0.41 sd(y-x)= 1.44 sdx= 3.73 sdy= 3.62 pcxy= 0.961
Wind Speed (m/s) CMOD5 Wind
Wind Speed (m/s) 3-hourly First-Guess
0
5
10
15
20
25
30
35

Figure 16

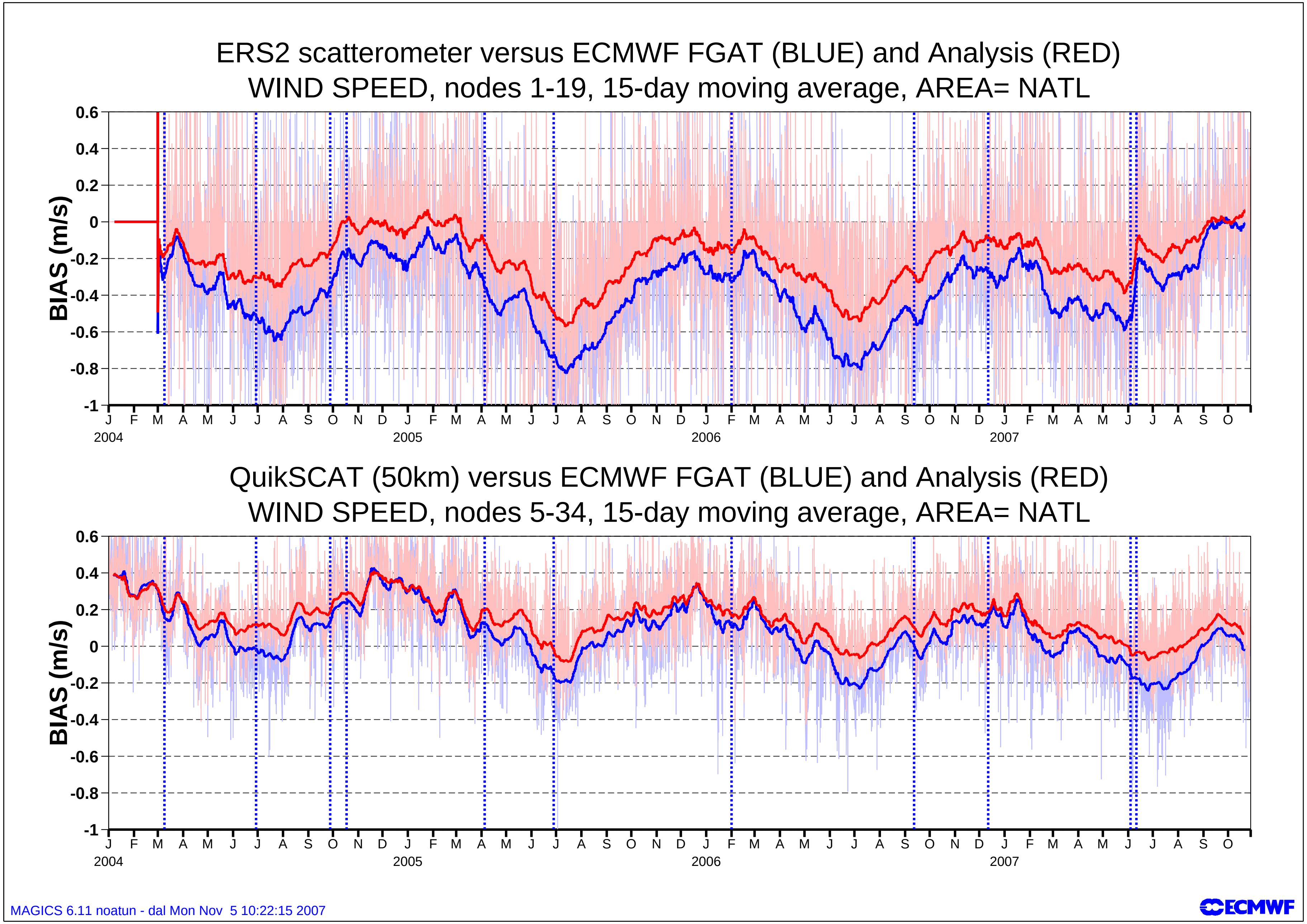
ERS2 scatterometer versus ECMWF FGAT (BLUE) and Analysis (RED)
WIND SPEED, nodes 1-19, 15-day moving average, AREA= NATL
BIAS (m/s)
0.6
0.4
0.2
0
-0.2
-0.4
-0.6
-0.8
-1
J F M A M J J A S O N D J F M A M J J A S O N D J F M A M J J A S O N D J F M A M J J A S O
2004
2005
2006
2007
QuikSCAT (50km) versus ECMWF FGAT (BLUE) and Analysis (RED)
WIND SPEED, nodes 5-34, 15-day moving average, AREA= NATL
BIAS (m/s)
0.6
0.4
0.2
0
-0.2
-0.4
-0.6
-0.8
-1
J F M A M J J A S O N D J F M A M J J A S O N D J F M A M J J A S O N D J F M A M J J A S O
2004
2005
2006
2007
MAGICS 6.11 noatun - dal Mon Nov 5 10:22:15 2007
ECMWF

Figure 17